PHYSICAL REVIEW B VOLUME 16, NUMBER 5 1 SEPTEMBER 1977

Theory of rare-earth alloys

Per-Anker Lindgård
Physics Department, Research Establishment Risø, DK-4000 Roskilde, Denmark
(Received 24 January 1977)

A mean-field random alloy theory combined with a simple calculation of the exchange interaction $J(c,Q)$ is shown to quantitatively account for the phase diagrams for alloys of rare-earth metals with Y, Lu, Sc, and other rare-earth metals. A concentration-dependent $J(c,Q)$ explains the empirical 2/3 law and reconstitutes the idea of de Gennes scaling. The phase diagrams exhibit examples of both *bicritical and tetracritical points*. No significant deviations from the mean-field calculation can be detected with the present experimental accuracy. A linear interpolation of $J(Q)$ for Gd and Er is found to account for all alloys except the Sc based. The exceptional behavior of the Sc alloys is due to a low density of states for Sc. A brief discussion is given of the effect on the mean-field results of changes in volume or c/a ratio and of critical fluctuations. Since the physical mechanisms of these ideal alloys are well documented they may serve as good candidates for studies of statistical effects such as multicritical phenomena or spin-glass phenomena.

I. INTRODUCTION

A wealth of experimental data exists on the alloys of rare-earth–rare-earth (RE) metals. Early reviews are given by Bozorth[1] and Rhyne[2]; further experiments have been performed later. The original reason for these studies was probably to get a deeper understanding of the physics of the pure RE. However, the alloy systems show several interesting examples of *multicritical points* at which transitions occur between different ordered phases as a function of temperature, concentration pressure, or magnetic field. Such *multicritical points* have recently been of great interest in the theory of critical phenomena.[3] If the physics of the RE alloys can be well understood, these may provide very good test examples for the theories of critical phenomena.

The physics of the RE metals were originally thought to be very simple. The exchange interaction between the total angular momentum J is the long-ranged Ruderman-Kittel-Kasuya-Yosida interaction, which was expected to scale with the de Gennes[4] factor $(g-1)^2$ from one element to the other. The anisotropies of the RE should scale with the Stevens factors[5] that determine the $4f$ electron distribution. Both the Landé factor g and the Stevens factors are determined by atomic calculations and independent of solid-state effects. However, the study of the RE alloys showed that, although this theory describes the gross features, very significant and systematic deviations occur. In particular it was found that for several RE alloys the Néel temperature T_N (which is proportional to the exchange interaction) did not vary linearly with the de Gennes factor, but rather followed an empirical $\frac{2}{3}$ law. The reason for this anomalous "universal" law, and in particular the marked exceptions represented by the Sc-based alloys, was not understood theoretically.[1]

In a recent paper,[6] referred to as I, the author showed that the phase diagrams of the RE alloys—also those with competing order parameters showing *tetracritical points*—could be understood qualitatively on the basis of the molecular-field theory and the original simple interaction picture. However, for an investigation of the effect of critical phenomena a quantitative understanding of the anomalous behavior is demanding. The purpose of this paper is to show that the deviation from the de Gennes scaling is due to a systematic and smooth variation of the band structure of the RE alloys that changes the Fourier-transformed exchange interaction $J(c,Q)$ as a function of concentration. The present arguments are based on a coherent-potential-approximation (CPA) treatment of the alloy problem. In effect the result is identical to the early phenomenological description by Wollan[7] where T_N is expanded in terms of a Fourier series; however, the interpretation is different. For a detailed understanding, the crystal field must be taken accurately into account. Use is here made of the recent crystal-field parameters by Touborg[8] and the Stevens factors. Two-ion anisotropy is not found to play any significant role.

In Sec. II the simple coherent-potential-approximation theory and the molecular-field theory are given, and the effects of the perturbations arising from changes in volume or c/a ratio and critical fluctuations are briefly discussed. Blackman and Elliott[9] have previously discussed the exchange interaction in concentrated alloys using a CPA calculation. However, their results are not easily applicable and their model Hamiltonian which only includes the difference in the local potentials is not likely to accurately describe the RE alloys. Com-

ments on this theory are given in Sec. II. Section III is a summary and discussion of the results of the comparison with several of the available phase diagrams of RE alloys. It is shown that these exhibit *bicritical* as well as *tetracritical points*.

II. SIMPLE THEORY OF ALLOYS WITH THE HEAVY-RARE-EARTH METALS

Since the heavy-rare-earth metals are chemically very similar, they form ideal alloys with each other and also with the rare-earth-like metals Y and Sc. All these alloys have three conduction electrons of predominantly d character per atom and form the hexagonal-close-packed structure. The magnetic properties are, however, very different, mainly because of the effect of the crystal field. The exchange interaction is the long-ranged Ruderman-Kittel-Kasuya-Yosida (RKKY), predominantly isotropic interaction. The Hamiltonian for the alloy is

$$\mathcal{H} = -\sum_{\substack{ij \\ np}} P_i(n)P_j(p)(g_n - 1)(g_p - 1) \times J_{ij}^{np}\vec{J}_{in}\cdot\vec{J}_{jp} + \sum_{in} P_i(n)V(J_n)\,, \tag{1}$$

where $P_i(m)$ is 1 or 0 if site i is occupied or unoccupied by atom type m, respectively; g_m is the Landé factor, J_m the total $4f$ angular momentum and $V(J_m)$ the crystal field acting on an atom of type m. For the long-ranged interaction, the temperature effect is well described by the molecular-field theory. The effect of critical fluctuations is considered later. For the same reason the virtual-crystal approximation used in I is quite good. This approximation implies that $P_i(m)$ is replaced by the configurational average, i.e., $P_i(m) \sim \bar{P}_i(m) = c_m$, the concentration of atom type m. However, we shall now consider the possibility that the exchange interaction may depend on the concentration. Such an effect may be caused by a change in the band structure as a function of concentration and can be accounted for by using the CPA.[10] As in I, the phase separation line between the paramagnetic and the ordered phase is obtained from the condition

$$[1/\chi^0_{\alpha\alpha,1} - cJ_{11}(c,Q)][1/\chi^0_{\beta\beta,2} - (1-c)J_{22}(c,Q)] = c(1-c)J_{12}^2(c,Q)\,, \tag{2}$$

where Q is the ordering wave vector and $\chi^0_{\alpha\alpha,1}$ is the noninteracting susceptibility of the $4f$ moment; $J_{ln}(c,Q) = 2\sum_R J_{ij}^{ln}(c)e^{i\vec{Q}\cdot\vec{R}ij}$ is twice the Fourier-transformed exchange interaction between elements of type l and n. Combining the RKKY and the CPA theory for the paramagnetic phase we obtain

$$J_{ln}(c,q) = \frac{1}{N}\sum_k j_l(k,k+q)j_n(k,k+q)\frac{f^c_k(1-f^c_{k+q})}{\epsilon^c_{k+q} - \epsilon^c_k} \tag{3}$$

$$\equiv j_l j_n \bar{\chi}_{el}(c,q)\,, \tag{4}$$

where ϵ^c_k are the alloy conduction-electron energies at the concentration c, $f_k = [e^{(\epsilon_F - \epsilon_k)/k_BT} + 1]^{-1}$ and $j_m(k,k+q)$ the $d-f$ matrix elements, assumed to be independent of c. In (4) we have approximated (3) by an averaged wave-vector-dependent electronic susceptibility function $\bar{\chi}_{el}(c,q)$ and with j_m being the effective $d-f$ matrix element determining the magnitude of the exchange interactions. For $q \to 0$, (4) reduces to the well-known approximation, since $\bar{\chi}_{el}(c, q\to 0) = \bar{\rho}_c(\epsilon_F)$, the density of states at the Fermi energy for the alloy. We now take advantage of the fact that the rare-earth elements are chemically very similar. Assuming that only the bandwidths are slightly different it is easy to show from the CPA equation that the dominant concentration dependence of the alloy susceptibility for the paramagnetic phase is given by the weighted average of the elemental susceptibilities.

$$\bar{\chi}_{el}(c,q) = c\bar{\chi}_1(q) + (1-c)\bar{\chi}_2(q)\,, \tag{5}$$

where $\bar{\chi}_m(q)$ is the averaged (with respect to the matrix elements) wave-vector-dependent susceptibility of the pure element of type m. The advantage of the simple expression (5) is that $\bar{\chi}_m(q)$ can either be taken from measurements or calculated from realistic band structures for the pure element. By expanding of the CPA equation in terms of the difference in the bandwidths relative to the average bandwidth corrections to (5) (of higher powers of c) can be generated. If the alloy elements are significantly different chemically (5) is no longer a good approximation. A CPA calculation of the RKKY interaction for this case is complicated[9] and conclusions have only been obtained based on numerical calculations using extreme approximations. The major general result is that the spin disorder scattering produces a finite mean free path λ for the electrons and therefore gives an asymptotic behavior of the RKKY interaction for large R as $e^{-R/\lambda}$ rather than as R^{-3}. However, this effect does not manifest itself strongly in the following applications to relatively high concentration alloys.

A. Alloys with a nonmagnetic metal

Let us first consider the alloys $Gd_{1-c}M_c$ of Gd with the nonmagnetic M = Y, Lu, and Sc of concentration c. Since Gd is an S-state ion, the crystal-field effect is very small and $\chi^0_{\alpha\alpha,Gd} = \frac{1}{3}S(S+1)/kT$, where $S = 3.5$ is the total spin of Gd. For simplicity, we neglect the effect of the conduction-electron polarization. The Curie and Néel temperatures are then simply obtained from

$$3kT = (1-c)S(S+1)J_{\mathrm{Gd\,Gd}}(c,Q) \tag{6}$$

for $Q=0$ and $Q\neq 0$, respectively.

At low concentrations of M (M = Y, Lu, and Sc) the magnetic structure is *ferromagnetic* with T_c given by

$$kT_c = \tfrac{1}{3}(1-c)S(S+1)j_{\mathrm{Gd}}^2 \times [c\bar{\rho}_M(\epsilon_F) + (1-c)\bar{\rho}_{\mathrm{Gd}}(\epsilon_F)]\,. \tag{7}$$

The experimentally found deviation from a linear relation between kT_c and c, which has been called the empirical $\frac{2}{3}$ law,[1,2] can thus be understood as an effect of a concentration-dependent band structure when $\bar{\rho}_M(\epsilon_F) \neq \bar{\rho}_{\mathrm{Gd}}(\epsilon_F)$. Figure 1 shows the fit to the existing experimental points obtained using (7). Y has very nearly the same atomic volume as Gd. However, for Sc and Lu it is smaller by 25% and 10%, respectively.

The change in volume can be taken into account as follows. We consider the RKKY interaction to be predominantly mediated by the d electrons as is the case in pure Gd. We assume that the bandwidth of the d electrons is approximately inversely proportional to the volume. This is substantiated by a detailed calculation using the canonical-band idea for Fe.[11] Since the canonical bands only depend on the structure (hcp), it follows that the density of states near the Fermi energy is proportional to the volume and thus has the concentration dependence

$$\bar{\rho}_i(V(c),\epsilon_F) \sim \frac{V(c)}{V(0)}\,\bar{\rho}_i(\epsilon_F) = \left(1 - c\frac{\Delta V}{V}\right)\bar{\rho}_i^0\,, \tag{8}$$

where $\Delta V/V = (V_{\mathrm{Gd}} - V_M)/V_{\mathrm{Gd}}$ is the relative volume change between Gd and M, $\bar{\rho}_i^0$ is the density of states at ϵ_F for the pure-element volume V_i. Taking this effect into account we find

$$kT_c = \tfrac{1}{3}(1-c)S(S+1)j_{\mathrm{Gd}}^2 \times [c(\bar{\rho}_M^0 - \Delta V/V\bar{\rho}_{\mathrm{Gd}}^0) + (1-c)\bar{\rho}_{\mathrm{Gd}}^0 + c^2(\Delta V/V)(\bar{\rho}_{\mathrm{Gd}}^0 - \bar{\rho}_M^0)]\,. \tag{9}$$

The correction is particularly important for Sc and Lu. As the coefficient to c^2 is small, (9) reduces effectively to (7). A slightly better fit could be obtained to (9) (not shown) than to (7) in Fig. 1. The deduced exchange interaction and densities of states are given in Table I assuming $\bar{\rho}_{\mathrm{Gd}}^0 = 2.0$ states/eV/atom, which gives $j_{\mathrm{Gd}} = 0.049$ eV (note that all subsequent parameters for the other alloys are determined relative to these values). The chosen Gd parameters were recently found to account for magnetic moments and transition temperatures in the $\mathrm{Gd}_{1-c}T_c$ (T = Co, Ni) alloys.[10]

At higher concentrations of M = Y, Lu, and Sc, the magnetic structure of the $\mathrm{Gd}_{1-c}M_c$ alloys is a

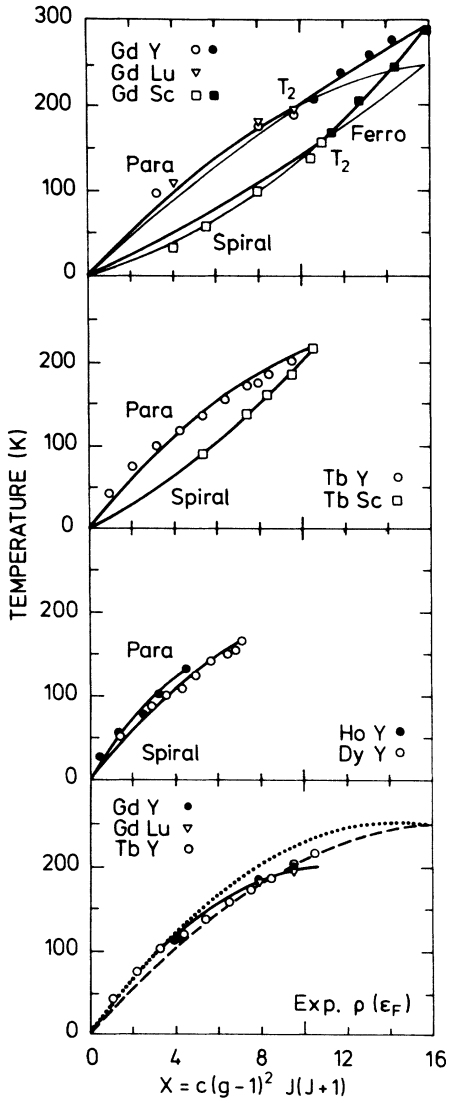

FIG. 1. Transition temperatures [reduced for the effect of the crystal field according to (12)] for rare-earth alloys with a nonmagnetic element. The heavy full line is the calculated phase line. The thin line is the continuation into the alternative phase. The Gd alloys show a *bicritical point* T_2 at which the order changes from ferromagnetic to spiral order as a function of the de Gennes factor X or the concentration. The last figure shows the phase lines calculated using the $\bar{\rho}(\epsilon_F)$ determined from specific-heat measurements (Ref. 14). —TbY, ···GDY, and --- GdLu.

spiral structure characterized by the ordering vector Q and the ordering temperature given analogously to (7) and (9) by

$$kT_N = \tfrac{1}{3}(1-c)S(S+1)j_{\mathrm{Gd}}^2[c\bar{\chi}_M(Q) + (1-c)\bar{\chi}_{\mathrm{Gd}}(Q)]\,, \tag{10}$$

where we have assumed the same d-f exchange matrix element, j_{Gd}. Since it is known that $Q = Q(c)$ is a function of concentration,[12] also $\bar{\chi}_i(Q(c))$ de-

TABLE I. First are given the basic physical properties of the elements composing the various alloys. Next come the effective matrix elements j_{df} deduced in the present analysis and the corresponding averaged electron susceptibilities $\bar{\chi}_N(Q)$ and $\bar{\chi}_c(0)$. As described in the text the values are normalized with respect to the Gd values. The total density of states at the Fermi energy $\rho(\epsilon_F)$, calculated from the APW energy bands, is shown for comparison. A is the simple crystal-field correction used in (12) and (13). The crystal-field parameters B_i^0 are given below. In the complete crystal-field calculations the B_2^0 derived from $\Delta\theta$ for the pure elements have been used.

	Gd	Tb	Dy	Ho	Er	Tm	Lu	Y	Sc	Comments
$4f$ electrons	7	8	9	10	11	12	14	0	0	Ref. 2
V cm^3/mol	19.91	19.30	19.03	18.78	18.49	18.14	17.79	19.95	15.04	Ref. 2
$r = c/a$	1.591	1.581	1.574	1.572	1.572	1.571	1.584	1.573	1.592	Ref. 2
j_{df} (eV)	0.049	0.051	0.051	0.051	0.049	0.050	0	0	0	This work
$\bar{\chi}_N(Q)\left(\frac{\text{states}}{\text{eV}}\right)$	1.71	2.06	2.29	2.76	3.00	2.67	3.02	3.02	1.7	This work
$\bar{\chi}_c(0)\left(\frac{\text{states}}{\text{eV}}\right)$	2.0	...	...	...	...	...	...	2.50	1.1	This work
$\rho(\epsilon_F)\left(\frac{\text{states}}{\text{eV}}\right)$	2.1	2.0	2.0	...	1.8	...	1.9	3.9	2.5	Band calculation (Refs. 17 and 18)
$\rho_{\text{exp}}\left(\frac{\text{states}}{\text{eV}}\right)$	2.0	2.4	...	...	...	...	3.7	4.4	...	From C_v relative to Gd (Ref. 14)
A (K)	0	15	16	5	13	45	...	...	...	
B_2^0 (K)	0	0.90	0.63	0.17	−0.39	−1.40	...	...	...	From $\Delta\theta$, Ref. 12
B_2^0 (K)	0	1.04	0.65	0.23	−0.26	−1.04	...	...	...	Dilute Y alloys (Ref. 8)
$B_4^0\times10^4$ (K)	0	8.61	−4.03	−2.26	3.02	11.1	...	...	...	...
$B_6^0\times10^5$ (K)	0	−1.52	1.04	−1.77	2.82	−7.62	...	...	...	...

pends on the concentration. This effect can be taken into account by a Taylor expansion in a way analogous to the volume effect leading from (7) to (9). T_N is therefore in general a polynominal expansion in c with effective parameters. A fit to (10) neglecting the higher-order terms in c^n is shown in Fig. 1, and the deduced electron susceptibility is given in Table I. Figure 2 shows a CPA calculation of the conduction-electron polarization. For Sc, the effect of the volume change is shown. We note the effective polarization per Gd atom is nearly independent of concentration.

Let us now consider the alloys $R_{1-c}M_c$ of R, a heavy-rare-earth metal, Tb or Dy, with the nonmagnetic M = Y, Lu, and Sc. Here, the orbital moment L of the $4f$ electrons is nonzero and this gives rise to crystal-field effects. At high temperatures, only the axial term $B_2^0O_2^0$ contributes and gives rise to a uniform separation between the inverse susceptibilities parallel and perpendicular to the hexagonal axis.

$$1/\chi_\perp(T) - 1/\chi_\parallel(T) = \theta_\perp - \theta_\parallel = \Delta\theta = \tfrac{3}{10}[4J(J+1)-3]B_2^0. \quad (11)$$

The transition temperature for the alloys influenced by the crystal field is therefore

$$k(T - A_R) = \tfrac{1}{3}(1-c)J_R(J_R+1)(g_R-1)^2 \times j_R^2[c\bar{\chi}_M(Q) + (1-c)\bar{\chi}_R(Q)], \quad (12)$$

where, for the planar rare-earth metals Tb, Dy, and Ho, $A_R = \frac{1}{3}\Delta\theta$, and for the axial rare-earth metals Er and Tm, $A_R = -\frac{2}{3}\Delta\theta$. The best fit to the

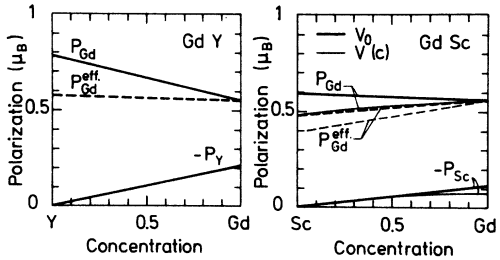

FIG. 2. Conduction-electron polarization calculated using the CPA theory. The polarization of Y and Sc is found to be antiferromagnetic relative to the Gd moment. P_{Gd}^{eff} is the effective polarization per Gd atom if the Y or Sc moment is assumed to be zero. The thin lines for the GdSc alloys include the effect of the different volumes for Gd and Sc. The general conclusion is that the CPA calculation predicts an almost constant P_{Gd}^{eff}.

experimental data is shown in Fig. 1. The effect of changes in volume and the spiral wave vector Q, is of course, analogous to that discussed for Gd.

B. Alloys of two rare-earth metals

The theory is easily generalized to alloys of two different magnetic rare-earth metals. Of particular interest are alloys of elements with competing order parameters; for example, the alloys of Tb and Tm. Tb prefers a spiral order with the moment perpendicular to the hexagonal axis and Tm a sinusoidal structure with the moments along the hexagonal axis. The different moment directions are due to crystal-field effects since for Tb: $1/\chi_{\parallel}^{0} > 1/\chi_{\perp}^{0}$, while for Tm: $1/\chi_{\perp}^{0} > 1/\chi_{\parallel}^{0}$. Assuming the B_2^0 contribution is dominant at high temperatures, we find from (2) the ordering temperature

$$3k_BT = \tfrac{1}{2}\{E_1 + E_2 + A_1 + A_2 + [(E_1 - E_2 + A_1 - A_2) + 4E_1E_2]^{1/2}\}, \quad (13)$$

where the anisotropy enters via

$$A_i = \Delta\theta_i \times \begin{cases} \pm 1/3 \\ \mp 2/3 \end{cases}$$

and the exchange interaction via $E_i = c_i(g_i - 1)^2 \times j_i^2 \bar{\chi}(c, Q)/J_i(J_i + 1)$. It is clear that (13) simplifies considerably for $A_1 = A_2$. For competing order parameters we find two phase separation lines as the solutions for

$$A_1 = \tfrac{1}{3}\Delta\theta_1, \quad A_2 = -\tfrac{2}{3}\Delta\theta_2, \quad (14a)$$

$$A_1 = -\tfrac{2}{3}\Delta\theta_1, \quad A_2 = +\tfrac{1}{3}\Delta\theta_2. \quad (14b)$$

However, for a detailed description at low temperatures ($T < 100$ K) we must take the complete crystal field into account. Using $\bar{\chi}(c, Q)$ as defined in (15), the basic equation (2) and the *complete level scheme* with the parameters given in Table I, we find, with only one adjustable parameter per element, the fits as shown in Fig. 3.

For the calculation of the (second-order) phase separation lines in the ordered phase, we again use (2) but with the susceptibilities calculated using the complete self-consistent level schemes in the presence of the molecular fields caused by the various ordered moments. We have not included extra terms in the crystal field present only in the ordered phase as for example the magnetoelastic effects. These are presumably quite important, but detailed knowledge of the magnetoelastic coupling constants is rather sparse. Perhaps a detailed analysis of the phase diagrams can improve this knowledge.

C. Refinements of the theory

In this section we consider corrections of the theory with respect to concentration-dependent

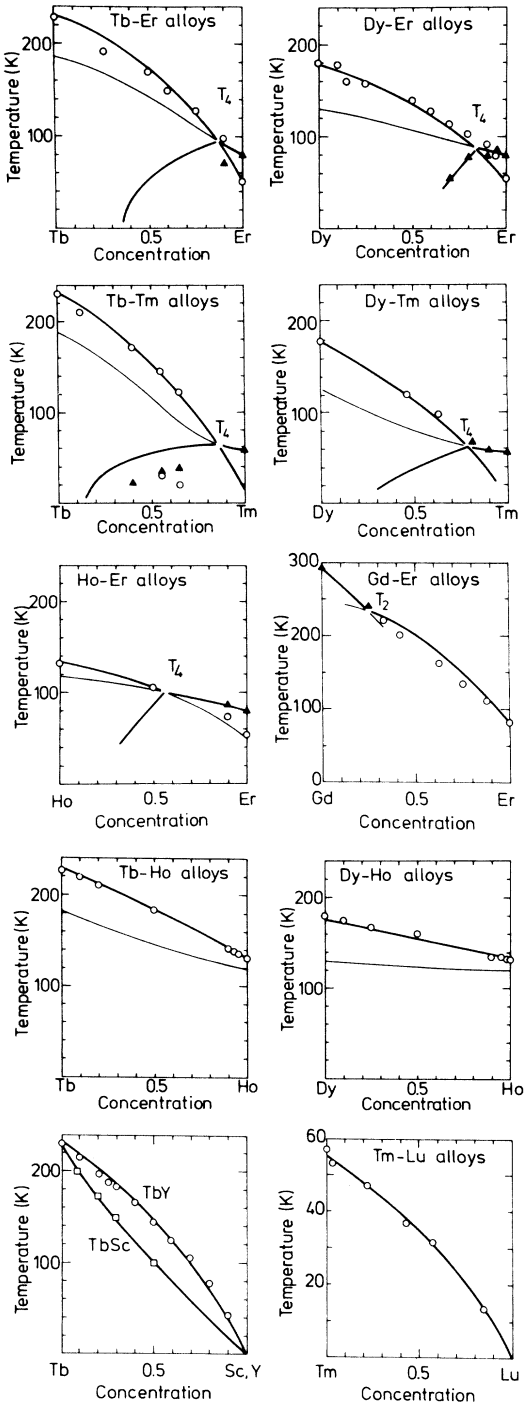

FIG. 3. Several phase diagrams for alloys of two different rare-earth metals. The crystal field is here included exactly. The GdEr alloys show a *bicritical point* T_2 and several alloys of elements with competing order parameters show a *tetracritical point* T_4. The parameters used are given in Table I. The heavy full line is the calculated phase line, the thin line is the continuation into the attenuation phase.

parameters and improvements of the molecular-field approximation. The effect on the exchange interaction of a concentration-dependent volume $V(c)$ per atom was already considered in the previous sections. The volume dependence of the dominant axial anisotropy parameter is opposite to that of the density of states (8):

$$B_2^0(V(c)) \sim B_2^0 V(0)/V(c) \sim B_2^0(1+c\Delta V/V). \tag{15}$$

A concentration dependence of the ratio between the c axis and the a axis $c/a = r$ has the following effect. The axial anisotropy is strongly dependent on $r(c)$:

$$B_2^0(r(c)) = B_2^0\left(1+\frac{3[r^2(0)-r^2(c)]}{8-3r^2(0)}\right). \tag{16}$$

The exchange interaction (i.e., the susceptibility) is expected to be less sensitive.

Finally we consider the effects of critical fluctuations. The predominant effect is to lower the critical temperature relative to that calculated by molecular-field theory T_c^{MF}. The effect depends on the anisotropy and is thus different for the Ising, x-y, and Heisenberg systems. However, to a good approximation the lowering can be assumed to be proportional to the transition temperature T_c. We can therefore include in a simple fashion the effects of critical fluctuations in the general molecular-field expression (13) by renormalizing the exchange interaction term

$$E_i = E_i^{\mathrm{MF}}/(1-\Delta T_i)$$

and the anisotropy term (17)

$$A_i = A_i^{\mathrm{MF}}(1-\Delta T_i),$$

where

$$\Delta T_i = (T_c^{\mathrm{MF}} - T_c^{\mathrm{true}})/T_c^{\mathrm{MF}}|_i \tag{18}$$

is the relative lowering of the transition temperature. As ΔT_1 can differ from ΔT_2, we see that within this approximation the molecular-field formula (13) is unchanged, only the parameters are to be interpreted as renormalized, Therefore the molecular-field approximation is expected to be a good approximation with respect to predicting the phase diagram, except perhaps for a region close to a tetracritical or bicritical point. Aharony[13] has recently argued on the basis of an ϵ expansion that the critical exponents should in fact be the molecular-field ones. A detailed test of this prediction would be of interest.

III. DISCUSSION AND COMPARISON WITH EXPERIMENTS

The theory has been compared with several of the available measurements.[1,2,12] If the theory is to make sense, the two adjustable parameters, j_{df} and $\bar{\chi}(Q)$, per alloy element should be specific for each element and independent of which particular alloy the element enters into. This is indeed the case and it is further found that j_{df} is essentially identical for the heavy-rare-earth metals $j_{df} \simeq 0.050$ eV. This effectively reduces the number of adjustable parameters to one per element.

Alloys with Y, Lu, or *Sc.*[2] The full line in Fig. 1 represents the calculated paramagnetic phase separation lines for the RE alloys with a nonmagnetic metal Y, Lu, or Sc. The Tb alloys have been corrected for the influence of the crystal field as in (12). The de Gennes theory[4] predicts a linear variation of the transition temperature with concentration. The convex curvature observed for Y and Lu is due to a higher conduction-electron susceptibility $\bar{\chi}(Q)$ than for Gd. The "universal" behavior of the heavy-RE–Y alloys is the result of an almost linear increase of $\bar{\chi}_R(Q)$ with increasing number of $4f$ electrons, Fig. 4. This is discussed in more detail below. By measurements[14] of the specific heat for Y and Lu, alternative densities of states at the Fermi energy $\bar{\rho}(\epsilon_F)$ can be deduced. The lower part of Fig. 1 shows the result of a calculated using these experimental $\bar{\rho}_Y(\epsilon_F)$ and $\bar{\rho}_{Lu}(\epsilon_F)$ and the j_{df} determined here. We conclude that these values are consistent with the $\bar{\chi}(Q)$ found here, in particular with respect to being much larger than the RE values, Table I. The concave curvature of the Sc-based alloys can, on the other hand, be understood as a result of a small $\bar{\chi}_{Sc}(Q)$. The volume correction (9) is important here. The uncorrected $\bar{\chi}_{Sc}(Q)$ is 40% and 25% smaller for ferromagnetic and antiferromagnetic ordering, respectively.

Alloys of two RE metals.[12] Having determined the parameters for Gd, Tb, Dy, and Ho, the remaining ones for Er and Tm are obtained from the phase diagrams for DyEr and TbTm. All other measured phase diagrams shown in Fig. 3 then agree, within the experimental accuracy, with the calculation using the given set of parameters, Table I. Here the full crystal field has been used. This slightly improves the fit for the TbY and TbSc alloys. We note that the *tetracritical points* for the Tb-Er, DyEr, TbTm, and Ho-Er are consistent with the experimental observations. In I the *ad hoc* increase of the interalloy element exchange interaction was sufficient to give overall agreement, but was unable to provide agreement in this respect.

Multicritical points are observed in several of the alloys. The *tetracritical point* in Dy-Er is the best documented experimentally. Good agreement with the molecular-field theory is obtained in the ordered phase. A more detailed experimental investigation close to the tetracritical region would

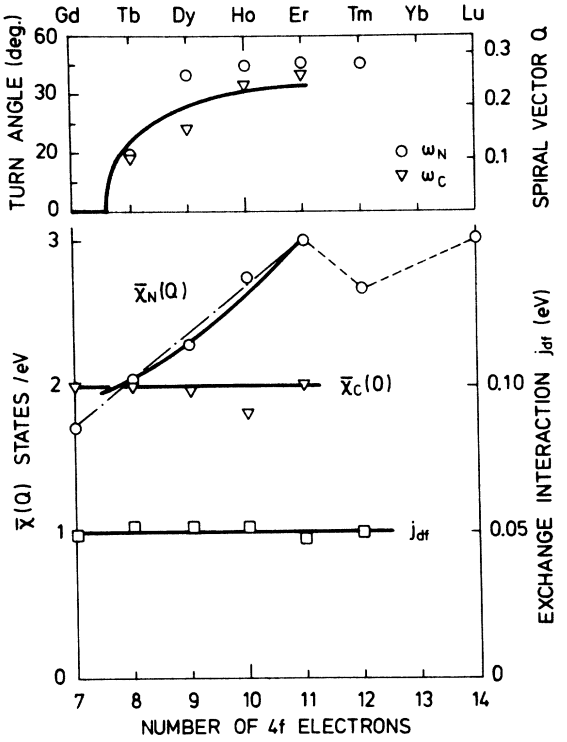

FIG. 4. At the top is shown the experimental variation of the spiral wave vector Q (turn angle ω), at the Néel temperature ○ and at the Curie temperature ▽. The full line represents the prediction based on the effective alloy exchange interaction $J_{\text{alloy}}(c,q)$, Fig. 5. On the lower right scale is shown the effective exchange matrix element j_{df}, which is essentially constant. The lower left scale and ○ show the presently found $\bar{\chi}_N(Q)$, the heavy full line is the predicted variation based on $J_{\text{alloy}}(c,q)$, Fig. 5. This variation is essentially linear between Gd and Er. From the experimental $\theta_{\parallel}$ and $\theta_{\perp}$ and j_{df} we deduce $\bar{\chi}_c(0)$ indicated by a ▽. This is nearly constant as expected by de Gennes. [It should be noted that j_{df} and $\chi(Q)$ are strongly correlated, as is clear from (6)–(13).]

be interesting in order to establish if the small deviations from the theory in this region are real. Well into the ordered phase we do not expect the calculations to be accurate since the magnetoelastic effects have been neglected. This may be the reason for the deviations observed in the Tb-Tm alloys. In general, however, the theory for transitions between the ordered phases is more complicated and it is probably necessary to treat the various possible intermediate fan structures, as discussed by Kitano and Najamiya.[15] The GdM alloys (M = Y, Sc, Lu, and Er) exhibit *bicritical points*. This is very unusual for alloy systems. The transition occurs between a ferro- and a spiral ordering as a function of concentration. This may be a first-order transition as can be seen in Fig. 5, which shows that the peak in the interpolated $J(Q)$ between Er and Gd gradually decreases as a function of concentration. $J_{\text{Er}}(q)$ and $J_{\text{Gd}}(q)$ are obtained from a recent analysis of spin-wave data.[16] At $c \sim 10\%$ Er, the maximum in $J(Q)$ may change discontinuously from $Q \sim 0.1$ to $Q = 0$. This is in reasonable agreement with the observed transition at around $c = 25\%$ for the GdEr alloys, Fig. 3.

Explanation of the universality. The following picture has evolved through the analysis of the numerous diagrams. The effective exchange matrix element j_{df} is essentially constant. However, the band structure gradually changes as the number of 4f electrons increases such that a peak in $\chi(Q)$ grows for finite Q and dominates a possible reduction by a q-dependent matrix element. This

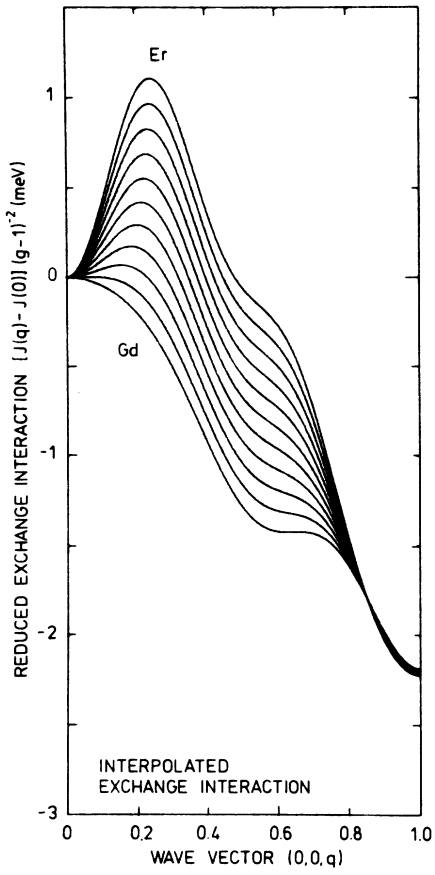

FIG. 5. Interpolated reduced exchange interaction $J_{\text{alloy}}(c,\vec{q}) = cJ_{\text{Gd}}(\vec{q}) + (1-c)J_{\text{Er}}(q)/(g_{\text{Er}}-1)^2$ for $\vec{q} = (0,0,(2\pi/c)q)$. We assume $J_{\text{Er}}(Q) = J_{\text{Y}}(Q)$ and $J_{\text{Lu}}(Q)$ as suggested by their equal, $\bar{\chi}(Q)$, Table I. The prediction based on this $J_{\text{alloy}}(c,\vec{q})$ is shown as the full heavy lines on Fig. 4, assuming a linear variation with the number of 4f electrons such that each electron corresponds to $\Delta c = 25\%$.

gives rise to a peak also in $J(Q)$ for finite Q. Calculations of $\chi(Q)$ (Ref. 17) from the APW bands[18] have been performed and they do indeed show this trend. Since the calculation of the exchange matrix elements[19] are still too complicated to give quantitative results for $J(Q)$,[20] we use the experimentally determined $J(Q)$. Arguments along this line were in fact given in Ref. 17. In Fig. 4 we have plotted the deduced j_{df}, $\bar{\chi}_N(Q)$, and the experimental $\bar{\chi}_c(0)$ obtained from $\theta_{\parallel}$ and $\theta_{\perp}$ using the same j_{df}. It is plausible to assume that the gradual change occurs between Gd and Er, and then remains constant for Lu and also Y. The $J(q)$ along the (001) direction is well documented for both Gd and Er.[21] Figure 5 shows $J_{\mathrm{Gd}}(q)$ and $J_{\mathrm{Er}}(q)/(g_{\mathrm{Er}}-1)^2$ and a linear interpolation between them ($T=0$) The variation of the peak height is shown as the full line $\bar{\chi}_N(Q)$ in Fig. 4, and the position Q (turn angle ω) is shown at the top of Fig. 4. Since the turn angle ω changes with temperature, the concentration or number of $4f$ electrons, the agreement is quite satisfactory. It is clear from Fig. 4 that $\bar{\chi}_c(0)$ is essentially constant. This means that the scaling idea of de Gennes[4] would in fact be very accurate if the spiral order did not take over. The experimentally observed ferromagnetic transition temperature T_c (Ref. 12) is entirely determined by crystal-field and magnetoelastic effects and therefore does not behave in a systematic fashion.

Wollan[7] noted that a striking systematic picture of the magnetic properties of the rare-earth intermetallics was obtained when plotted as a function of the c/a ratio. The reason for this dependence is not obvious. The variations in the c/a ratio are most likely caused by the same effect that makes the band structure vary gradually as a function of the number of $4f$ electrons. The close similarity with Y is probably a coincidence. Sc is found to be much more different from Y than expected from the energy band calculations.[17] Such a difference was also noted in the phonon spectrum for Y and Sc.[17]

IV. CONCLUSION

The exchange interaction $J(q)$ for the pure heavy-rare-earth (RE) metals and alloys is a smoothly varying function between Gd and Er, whereas the effective matrix element j_{df} is essentially constant. $J(q)$ for the nonmagnetic Y and Lu is likely to be the same as for Er. This is in agreement with calculations based on the RE band structures and with the observed transition temperatures and variations in the spiral vector. This behavior explains the empirical $\frac{2}{3}$ law and supports the idea of de Gennes scaling. The deduced parameters are given and are in good agreement with those available from other measurements. The alloy phase diagrams show examples of *bicritical and tetracritical points*. The predictions of the mean-field–alloy theory agree with the observations within the experimental uncertainty. More detailed experiments in the region near the multicritical points in for example Dy-Er (tetracritical point caused by change in single-ion anisotropies) or Gd-Y (bicritical point caused by change in ordering wave vectors) would be of interest. Experimentally, the concentration is an unfortunate variable, which is not easy to vary continuously. However, because most of the rare-earth alloys order with a general wave vector, it is possible to shift the position (c, T) of a multicritical point by applying a uniform magnetic field. Therefore for a given, near critical, concentration it should be possible to obtain a detailed map of the multicritical region in an H, T plane.

ACKNOWLEDGMENT

It is a pleasure to thank B. Szpunar for assisting with some of the numerical calculations.

[1] R. M. Bozorth, J. Appl. Phys. 38, 1366 (1967).
[2] J. J. Rhyne, in *Magnetic Properties of Rare Earth Metals*, edited by R. J. Elliott (Plenum, London, 1972), p. 129.
[3] A. D. Bruce and A. Aharony, Phys. Rev. B 11, 478 (1975), and references therein.
[4] P. G. de Gennes, C. R. Acad. Sci. (Paris) 247, 1836 (1966).
[5] K. W. H. Stevens, Proc. Phys. Soc. A 65, 209 (1952).
[6] P.-A. Lindgård, Phys. Rev. B 14, 4074 (1976); AIP Conf. Proc. 29, 441 (1975).
[7] E. O. Wollan, J. Appl. Phys. 38, 1371 (1967).
[8] P. Touborg (unpublished); and J. Høg and P. Touborg, Phys. Rev. B 9, 2952 (1974).
[9] J. A. Blackman and R. J. Elliott, J. Phys. C 3, 2066 (1970).
[10] B. Szpunar and P.-A. Lindgård, Phys. Status Solidi 82, 1977); and B. Szpunar and B. Kozarzewski, Phys. Status Solidi 82, (1977).
[11] J. Madsen and O. K. Andersen, AIP Conf. Proc. 29, 327 (1975), and references therein.
[12] W. C. Koehler, in Ref. 2, p. 81; and TbTm by P. Hansen and B. Lebech, J. Phys. F 6, 2179 (1976).
[13] A. Aharony and S. Fishman, Phys. Rev. Lett. 37, 1587 (1976).
[14] P. Wells, P. C. Lanchester, D. W. Jones, and R. G. Jordon, J. Phys. F 4, 1729 (1975); 6, 11 (1976).
[15] Y. Kitano and T. Nagamiya, Prog. Theor. Phys. 31, 1 (1964).
[16] P.-A. Lindgård, Phys. Rev. B (to be published).
[17] S. H. Liu, R. P. Gupta, and S. K. Sinha, Phys. Rev. B 4, 1100 (1971); and P.-A. Lindgård, in *Magnetism*

in Metals and Metallic Compounds, edited by J. T. Lopuszanski, A. Pekalski, and J. Przystawa (Plenum, New York, 1976), p. 203.
[18]S. C. Keeton and T. L. Loucks, Phys. Rev. 168, 672 (1968).
[19]B. N. Harmon and A. J. Freeman, Phys. Rev. B 10, 4849 (1974).
[20]P.-A. Lindgard, B. N. Harmon, and A. J. Freeman, Phys. Rev. Lett. 35, 383 (1975).
[21]W. C. Koehler, H. R. Child, R. M. Nicklow, H. G. Smith, R. M. Moon, and J. W. Cable, Phys. Rev. Lett. 24, 16 (1970); A. D. B. Woods, T. M. Holden, and B. M. Powell, *ibid.* 19, 908 (1967); and R. M. Nicklow, N. Wakabayashi, M. K. Wilkinson, and R. E. Reed, *ibid.* 27, 334 (1971).